Journal of Catalysis 266 (2009) 71–78

Contents lists available at ScienceDirect

Journal of Catalysis

journal homepage: www.elsevier.com/locate/jcat

Catalytic coupling of carboxylic acids by ketonization as a processing step in biomass conversion

Christian A. Gaertner, Juan Carlos Serrano-Ruiz, Drew J. Braden, James A. Dumesic *

University of Wisconsin-Madison, Department of Chemical and Biological Engineering, Madison, WI 53706, USA

ARTICLE INFO

Article history:
Received 25 February 2009
Revised 20 April 2009
Accepted 15 May 2009
Available online 10 June 2009

Keywords:
Biomass conversion
Ketonization
Esterification
Hexanoic acid
Ceria–zirconia
Kinetic modeling

ABSTRACT

Carboxylic acids, common intermediate products in biomass conversion processes, can be converted into ketones via ketonization reactions over a ceria–zirconia catalyst. Reaction kinetics studies were carried out using hexanoic acid, as a representative carboxylic acid, in the presence of 1-pentanol and 2-butanone, as representative biomass-derived alcohol and ketone species. Studies were carried out at temperatures from 448 to 623 K, and employing a range of hexanoic acid partial pressures from 0.05 to 0.3 atm. Two different reactions were observed to take place at these reaction conditions: esterification and ketonization, both consuming hexanoic acid. Product inhibition by water and carbon dioxide was observed and studied by co-feeding these components to the reactor. Hexanoic acid adsorption on the catalyst surface is an important step in the reaction, and the rate of ketonization shifts from second order to zero order as the partial pressure of acid increases. The measured activation energy for the ketonization of hexanoic acid (132 kJ/mol) is higher than the esterification reaction (40 kJ/mol), such that the irreversible ketonization reaction is favored at higher temperatures (>573 K) compared to the reversible esterification reaction. Direct ketonization of esters does not take place in the presence of acids, and instead takes place by hydrolysis with water followed by ketonization of the corresponding acid. The results of this study can be described by a simple kinetic model including site blocking by adsorbed hexanoic acid, carbon dioxide, and water.

1. Introduction

The utilization of renewable resources for the substitution of fossil fuels is a key issue in moving our economy toward a more sustainable future [1]. In this respect, biomass is currently the only sustainable source for organic carbon [2]; however, the production of renewable fuels from biomass necessitates the development of new efficient processes to convert the biomass-derived feedstocks into liquid fuels [3,4]. The high functionality and corresponding reactivity of renewable carbohydrate feedstocks (i.e., high oxygen to carbon stoichiometry) compared to petroleum feedstocks requires alternative catalytic processing techniques to convert these resources into fuels for use in the transportation sector (e.g., gasoline, diesel, and jet fuels). We have recently reported a strategy to transform two important biomass-derived carbohydrates (glucose and sorbitol) into hydrocarbons of different classes to be used as transportation fuels [5]. This approach involves a two-step process in which the oxygen content of the feedstock is first reduced over a Pt–Re/C catalyst to generate monofunctional intermediates such as alcohols, ketones, and carboxylic acids in the C_4 to the C_6 range that spontaneously separate from water. In a subsequent step, these functional intermediates are upgraded by C–C coupling reactions into larger compounds. In this respect, the carboxylic acids and esters can be converted into heavier ketones via ketonization reactions, involving the condensation of two molecules of acid (or ester) to produce a linear ketone with $2n-1$ carbon atoms, CO_2, and water [6–9]. Use of this reaction as a means of reacting organic acid is of particular importance because biomass-derived organic effluents can possess a high content of carboxylic acids (e.g., as high as 30 wt% when glucose is used as reactant [5]).

In the present study, kinetic factors have been investigated for ketonization upgrading processes over a $Ce_{0.5}Zr_{0.5}O_2$ catalyst. This material showed desirable catalytic properties for ketonization of carbohydrate-derived carboxylic acids in the presence of other monofunctional oxygenated species [5] and thus was selected for further study. As a model for monofunctional organic effluents obtained in our previous work [5], we have studied the ketonization of hexanoic acid in mixtures with 1-pentanol and 2-butanone. Under the condition of this study, two primary reactions can proceed in parallel: (i) the reversible esterification of hexanoic acid and 1-pentanol to generate 1-pentylhexanoate (reaction (1)), and (ii) the ketonization of hexanoic acid to produce 6-undecanone, carbon dioxide, and water (reaction (2)).

* Corresponding author.
E-mail address: dumesic@engr.wisc.edu (J.A. Dumesic).

0021-9517/$ - see front matter © 2009 Elsevier Inc. All rights reserved.
doi:10.1016/j.jcat.2009.05.015

Hexanoic acid + 1-Pentanol ↔ 1-Pentylhexanoate + Water (1)

Hexanoic acid + Hexanoic acid → 6-Undecanone + Carbon Dioxide + Water (2)

We have studied the effects of solvents, partial pressures of the reactants and products, and reaction temperature on the rates of ketonization and esterification reactions. Additionally, we have investigated the inhibiting effects of carbon dioxide and water (produced by ketonization) on the kinetics of esterification and ketonization reactions. We have also studied the possibility for direct ketonization of esters to form the ketone adduct and CO_2, plus the stoichiometric alcohol and olefin. Finally, a simple kinetic model is presented that incorporates these effects to give a satisfactory description of the experimental results.

2. Experimental

A $Ce_{0.5}Zr_{0.5}O_2$ catalyst was prepared by a co-precipitation method described in detail elsewhere [10] using aqueous solutions of $Ce(NO_3)_3 \cdot 6H_2O$ (Aldrich, 99%) and $ZrO(NO_3)_2$ (Aldrich, 99%). Pure ZrO_2 oxide was prepared using the same method. Temperature programmed desorption of NH_3 and CO_2 was used to probe the acid and base sites, respectively, on these two catalysts, using an apparatus described elsewhere [11].

The reactor used for the reaction kinetic studies (Fig. 1) was a fixed-bed, upflow reactor consisting of a 6.35 mm outer-diameter tubular stainless steel tube (wall thickness 0.71 mm) containing the catalyst bed between two plugs of quartz wool (Alltech) and fused SiO_2 granules (Sigma–Aldrich). The reactor was heated with a close-fitting aluminum block heated externally by a well-insulated furnace (Applied Test Systems Inc.). Temperature was measured using a K-type thermocouple (Omega) attached to the outside of the reactor and controlled with a 1600 series type temperature controller (Love controls Series 16A). A mass-flow controller (5850 Brooks Instruments) was used to control the helium or carbon dioxide flowrates. A HPLC pump (Alltech 301 HPLC pump) was used to introduce the liquid feed solution into the reactor. The effluent liquid was collected at room temperature in a gas–liquid separator and drained for gas chromatography (GC) analysis (Shimadzu GC-2010 with a FID detector and Rtx-5 column) and identification (Shimadzu GC-2010 with a mass spectrometer and Rtx-5 column). The effluent gas stream passed through a back-pressure regulator (GO Regulator, Model BP-60) which controlled the system pressure. Gas phase samples were analyzed with two different GCs (Varian Star 3400 CX with a FID detector and a GS-Q capillary column for organic components and Shimadzu GC8A with a TCD detector and a HAYESFP DB100/120 column for the carbon dioxide measurements). All the feeds were prepared from high purity chemicals: hexanoic acid (99%, Aldrich), 2-butanone (99%, Aldrich), propyl hexanoate (Aldrich, ⩾98%), hexane (95%, Aldrich), and 1-Pentanol (⩾99%, Aldrich).

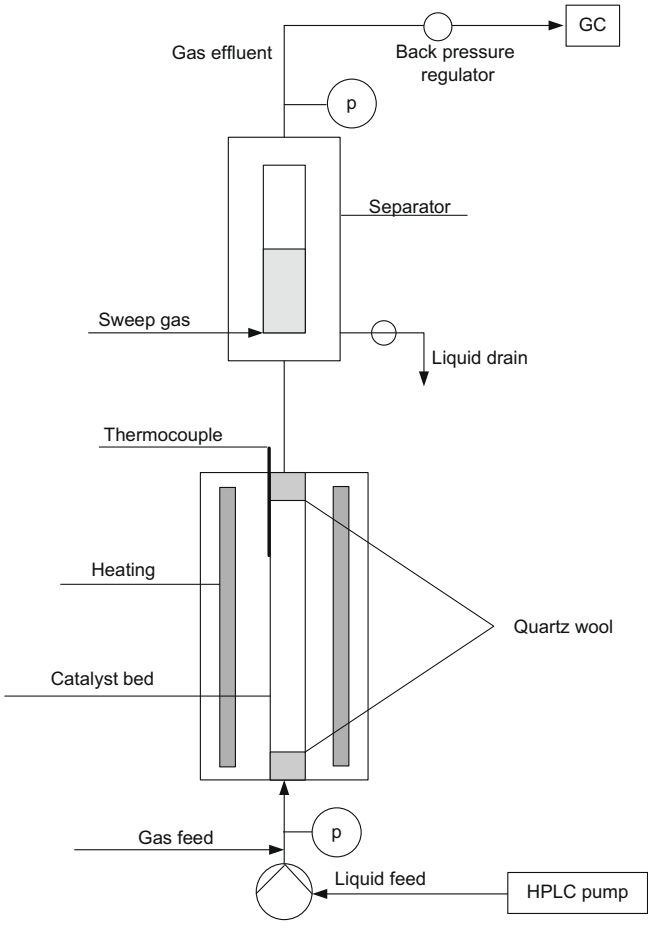

Fig. 1. Reactor setup used for reaction kinetics experimental studies.

3. Results

Experiments were carried out to determine the suitability of using 2-butanone as solvent for the kinetic studies of the ketonization of hexanoic acid. In this respect, 2-butanone was selected as the preferred solvent used to simulate the monofuctional organic effluent obtained in our original work [5] and these results were compared with those obtained using hexane as a solvent. Fig. 2 shows the ketonization rates (in terms of 6-undecanone and CO_2 formation) for a mixture of 7.5 mol% of hexanoic acid in both solvents at three different temperatures at a total pressure of 1 atm. It can be seen that the ketonization rates have similar values for both solvents at each of the three temperatures. Additionally, no reaction products aside from undecanone, CO_2, and water from the ketonization process were detected when 2-butanone was used as a solvent, and this ketone can thus be considered to be essentially inert over the ceria–zirconia catalyst at the conditions of the present study.

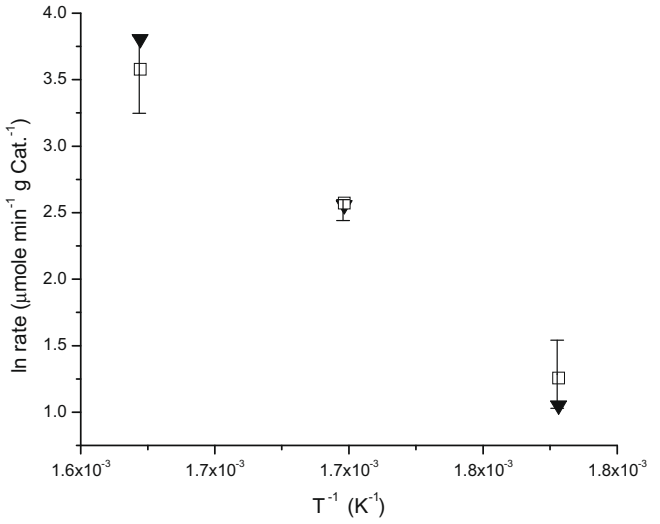

Fig. 2. Hexanoic acid ketonization reaction rates at various temperatures for a 7.5 mol% hexanoic acid feed using (▼) 2-butanone and (□) hexane as solvent.

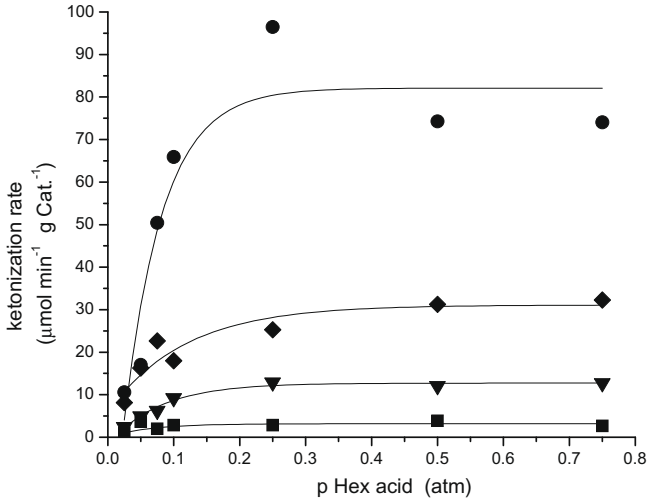

Fig. 3. Ketonization reaction rates for varying partial pressures of hexanoic acid using 2-butanone as solvent at (■) 547 K, (▼) 572 K, (♦) 597 K, and (●) 623 K.

Fig. 3 shows the ketonization rate at various temperatures (547–623 K) as a function of the partial pressure of hexanoic acid in the reactor at a total pressure of 1 atm. It can be seen that the ketonization rate reaches an asymptotic value with an increase in the hexanoic acid partial pressure in the reactor. The partial pressure where this limit is approached begins at approximately 0.1 atm. In order to study the effect of the presence of carboxylic acids and alcohols on the kinetics of simultaneously occurring esterification and ketonization reactions, experiments were performed at varying temperatures (448–623 K) at a total pressure of 1 atm and partial pressures of hexanoic acid and 1-pentanol, using different mixtures of these compounds in 2-butanone. The weight hourly space velocity (WHSV) for each experiment was varied to maintain the conversion below 60%. For all feeds listed in Table 1, a temperature study was performed, and the individual esterification and ketonization reaction rates were determined. Results are presented in Figs. 6–9, where the results of the kinetic model, discussed below, are also shown.

To check for the possible formation of the condensed ketone by the direct ketonization of the esters, a pure ester, propyl hexanoate, was fed to the reactor and reacted over ceria–zirconia. This experiment was performed by co-feeding helium to the reactor instead of using 2-butanone, since this organic solvent may contain traces of water which could lead to hydrolysis of the ester to an acid, followed by ketonization of the acid. As a comparison, we also studied the ketonization of pure hexanoic acid at the same conditions (623 K, 6.8 cm^3(STP) min^{-1} helium flow, 0.18 ml min^{-1} hexanoic acid or ester flow) leading to an acid/ester partial pressure of 0.026 atm at a total pressure of 1 atm. The ketonization rate for hexanoic acid (71 μmol min^{-1} g cat^{-1}), measured as the rate of undecanone formation, was then compared to the ketonization of propyl hexanoate (31 μmol min^{-1} g cat^{-1}). Interestingly, in both cases CO_2 was detected in the gas effluent while, when propyl hexanoate was used as a feed, 1-propanol in the liquid phase and propylene in the gas effluent were also found.

Since CO_2 and water are both products from the ketonization reaction, experiments were carried out to investigate the potential inhibiting effects of these compounds on the rates of esterification and ketonization. Thus, in the case of carbon dioxide, experiments similar to the those described above were performed with a gas co-feed through the reactor bed at a temperature of 598 K at a total pressure of 1 atm with a liquid feed composed of 7.5 mol% hexanoic acid in 2-butanone at a flow of 0.1 ml min^{-1} and a gas co-feed with varied composition at 42 cm^3(STP) min^{-1}. The total molar flow of the gas feed through the reactor was kept constant, and the molar ratio between helium and CO_2 was varied. As can be seen in Table 2, the ketonization rate decreased to approximately 29% of the initial value with a co-feed of CO_2 (runs K2-C and K3-C in Table 2). In order to check the reversibility of the CO_2 inhibition effect, a second run (K4-C) was carried out at the same conditions of the initial experiment (K1-C). It can be seen that the ketonization rate increased (4.8 versus 3.5 μmol min^{-1} g cat^{-1}) compared to the CO_2 co-feed experiments (K2-C and K3-C), but the initial ketonization catalytic activity (12.6 μmol min^{-1} g cat^{-1}) was not regained.

To investigate the CO_2-inhibiting effect for the esterification reaction, experiments were carried out by co-feeding CO_2 at a temperature of 548 K at a total pressure of 1 atm with a feed of 10 mol% hexanoic acid and 15 mol% 1-pentanol with 2-butanone as solvent (E1-C, E2-C, and E3-C shown in Table 2) at a liquid flow rate of 0.15 ml min^{-1} with a gas feed of varied composition at 45.6 cm^3(STP) min^{-1}. In contrast to the ketonization reaction, the esterification reaction rate was not significantly affected by the presence of CO_2 in the reactor.

The inhibiting effect of water on the ketonization reaction was investigated by carrying out experiments at varying concentrations of water in the feed (up to 5 wt%) while the concentration of the hexanoic acid was kept constant at 7.5 mol% (Table 3). A significant inhibiting effect of water on the hexanoic acid ketonization rate was observed (17.7 versus 6.7 μmol min^{-1} g cat^{-1}) when co-feeding only 5 mol% of water in the hexanoic acid and 2-butanone mixture.

The results presented above show that esterification and ketonization reactions take place simultaneously over ceria–zirconia. To assess the functionality of this catalyst, we carried out TPD experiments, using NH_3 and CO_2 to probe the acid and base sites, respectively. After integration of the desorption peak areas, $Ce_{0.5}Zr_{0.5}O_2$ showed a higher number of basic sites

Table 1
Feed mixtures for reaction kinetics studies.

Feed No.	mol%			WHSV range h^{-1}	
	Hexanoic acid	1-Pentanol	2-Butanone	Lower	Upper
1	0.10	0.10	0.80	3.5	19.7
2	0.05	0.10	0.85	3.5	19.9
3	0.10	0.05	0.85	3.5	19.7
4	0.15	0.10	0.75	3.5	20.1
5	0.10	0.15	0.75	3.5	19.7
6	0.20	0.10	0.70	3.4	19.5
7	0.10	0.20	0.70	3.5	19.7
8	0.30	0.10	0.60	3.6	20.4
9	0.10	0.30	0.60	3.5	19.8

Table 2
Effect of carbon dioxide on reaction rates (*E* = esterification at 548 K, *K* = ketonization at 598 K).

Run	mol% CO_2 gas feed	Rate ketonization (μmol min^{-1} g cat^{-1})	Run	mol% CO_2 gas feed	Rate esterification (μmol min^{-1} g cat^{-1})
K1-C	0.0%	12.6	E1-C	0.0%	6.2
K2-C	28.3%	3.5	E2-C	30.8%	7.0
K3-C	55.5%	3.7	E3-C	54.2%	8.9
K4-C	0.0%	4.8			

Table 3
Effect of water on ketonization rate (at 598 K).

Run	mol% water in solvent	Rate ketonization (μmol min^{-1} g cat^{-1})
K1-W	0.0%	17.7
K2-W	2.5%	10.2
K3-W	5.0%	6.7

(380 μmol g cat^{-1}) than acidic sites (56 μmol g cat^{-1}). Conversely, pure ZrO_2 showed a considerable number of acidic (212 μmol g cat^{-1}) and basic sites (296 μmol g cat^{-1}). This increased number of acidic sites for zirconia compared to those for ceria–zirconia is consistent with the literature [12]. To address the role of acid and base sites for the esterification and ketonization reactions, we then carried out selected reaction kinetics studies over the more acidic zirconium oxide catalyst. Thus, feed 1 (Table 1) was reacted over ZrO_2 at temperatures between 548 and 623 K. A noticeable increase in the rate of esterification (about 2 times higher than ceria–zirconia) was observed for this catalyst, while the ketonization rate was not significantly affected.

4. Discussion

The results shown in Fig. 2 suggest that 2-butanone does not inhibit the catalytic activity for the ketonization and esterification reactions. Accordingly, surface sites do not appear to be highly covered by species derived from 2-butanone. A second-order dependence of the ketonization reaction is observed with respect to the partial pressure of hexanoic acid, for partial pressures between 0 and 0.1 atm. For partial pressures greater than 0.1 atm, the reaction rate follows a zero-order dependence, suggesting that the catalyst sites are highly covered by species derived from hexanoic acid.

The experiments using propyl hexanoate as a feed showed the formation of 1-propanol and propylene. This result suggests that there is a direct mechanism for the conversion of esters to ketones, producing carbon dioxide, alcohol, and propylene. Different mechanisms have been proposed for this direct conversion of esters [13,14], involving various intermediates and products, such as alkenes. Importantly, the signature for this direct conversion is the formation of olefins. In our experiments using 1-pentanol and hexanoic acid as the feed, the conversion of the pentyl hexanoate formed by esterification could follow this direct ketonization route, as shown in Fig. 4, thereby forming pentene. However, because measurable amounts of pentene were not observed under our reaction conditions, it appears that the direct ketonization of esters does not take place in our system. Thus, we only consider two reactions (esterification and ketonization) as part of the reaction network used to describe our experimental data. The absence of the direct ketonization of esters in our experiments may result from the stronger adsorption of acids on the catalyst, thereby inhibiting the direct ketonization of esters in the presence of acids.

The TPD results show that $Ce_{0.5}Zr_{0.5}O_2$ possesses a mixture of basic and acid sites, with the former being more abundant on its surface, in agreement with previous work [15]. Whereas basic sites are needed for ketonization to take place [6,16–18], esterification reactions are commonly carried out over acidic catalysts [19–21]. Consequently, we assume that ketonization (basic sites) and esterification (acid sites) are catalyzed by different types of sites over ceria–zirconia. This assumption is justified by the fact that the esterification rates increase when zirconia oxide, which has more acidic sites, is used as a catalyst.

Possible product inhibition by CO_2 has to be taken into consideration for the results of the present study, because CO_2 adsorbs strongly on basic sites of ceria–zirconia oxide [15]. The results of this study, in fact, show strong inhibition of the rate of ketonization by adsorbed CO_2 (Table 2). In contrast, we have observed that esterification is not inhibited by CO_2, which supports our assumption that esterification does not take place on basic sites of ceria–zirconia, but rather that it takes place over acid sites.

Experiments carried out by co-feeding water to the reactor showed an inhibiting effect of water on the ketonization rate (Table 3). The strong adsorption of water on ceria–zirconia is reported elsewhere [22,23]. For the kinetic model it is assumed that water blocks the basic sites that are required for the ketonization, whereas water inhibition is not important for the esterification reaction. However, inhibition of the ketonization rate by adsorbed water does not appear to be as significant compared to the inhibiting effect of CO_2 adsorption.

The rate of ketonization exhibits a strong temperature dependence. Activation energies and pre-exponential factors for ketonization and esterification reactions can be determined with Arrhenius-plots, using experiments with the same feed composition. Fig. 5 shows the Arrhenius plot of the rate data obtained using Feed 1 (Table 1). The activation energy values determined were 28 and 134 kJ/mol for the esterification ketonization reactions, respectively. These values are used as initial guesses in our kinetic modeling described below.

A simple kinetic model was developed to describe the reaction kinetics for the combined ketonization and esterification reactions occurring on the ceria–zirconia catalyst. Previous studies [6,13] have investigated the ketonization mechanism using various techniques, and agreement about the detailed mechanism has not been found yet [24]. Thus, in the present study we use simple rate expressions to capture the essential aspects of the reaction kinetics. The ketonization reaction is modeled as an irreversible reaction

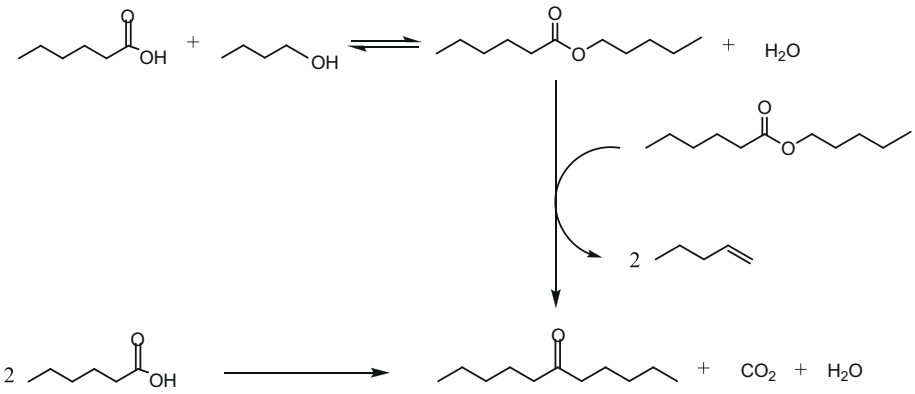

Fig. 4. Reaction network for esterification, ketonization, and ester-ketone transformation.

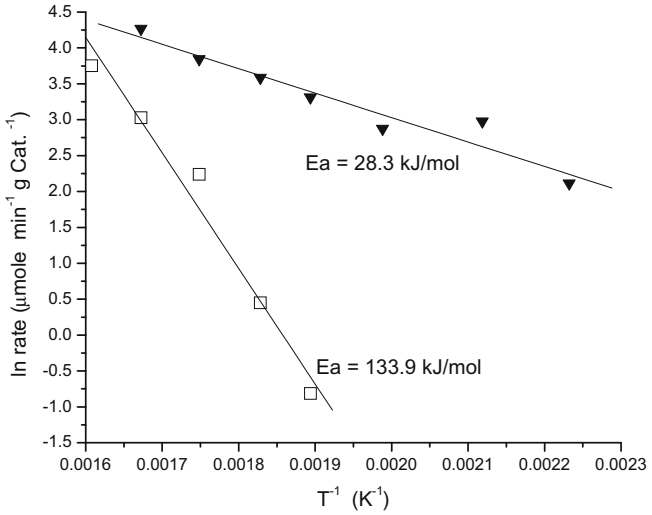

Fig. 5. Arrhenius plot for conversion of Feed Mix 1 for (▼) esterification and (□) ketonization reactions.

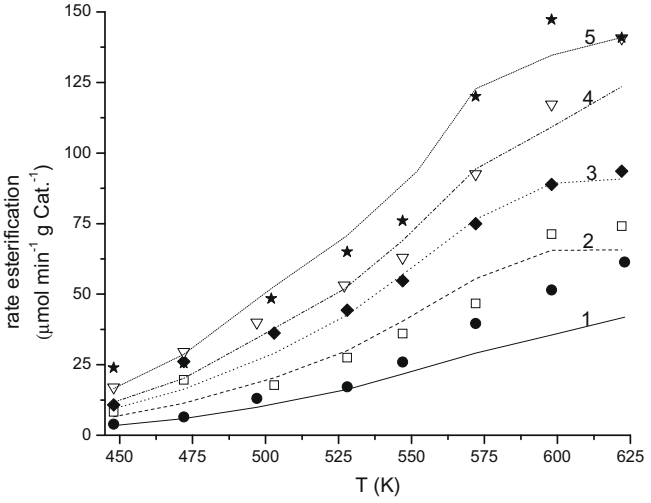

Fig. 6. Experimental (exp) data and simulation (sim) results for ester formation, partial pressure of hexanoic acid (hex ac) varied, partial pressure of 1-pentanol constant at 0.1 atm: (●) 0.05 atm hex ac exp, (1) 0.05 atm hex ac sim, (□) 0.1 atm hex ac exp, (2) 0.1 atm hex ac sim, (♦) 0.15 atm hex ac exp, (3) 0.15 atm hex ac sim, (▽) 0.2 atm hex ac exp, (4) 0.2 atm hex ac sim, (★) 0.3 atm hex ac exp, (5) 0.3 atm hex ac sim.

in which two adsorbed hexanoic acid molecules react to form 6-undecanone, adsorbed carbon dioxide, water, and a vacant catalyst site. Because of the release of carbon dioxide, the equilibrium constant for this process is high and the reaction can be assumed to be irreversible. The rates of adsorption and desorption for all gas phase species are assumed to be quasi-equilibrated. Therefore, the fractional surface coverage for species j, θ_j, can be written as Eq. (3), where $K_{ads,j}$ is the adsorption equilibrium constant for species j, and P_j is the partial pressure of species j. The fraction of vacant catalyst sites is expressed through the sum of species covering the catalyst surface subtracted from one. This site balance is used for the basic sites of the ceria–zirconia catalyst.

$$\theta_j = K_{ads,j} P_j \left(1 - \sum_j \theta_j\right) \tag{3}$$

The experimental results (Fig. 3 and Tables 2 and 3) suggest that hexanoic acid, CO_2, and water have a detrimental effect on the ketonization rate. In this respect, carbon dioxide and water are known to adsorb strongly on ceria–zirconia [12,15,22,23], and the ketonization rate has previously been found to be dependent on the acid coverage on the surface of the catalyst [25]. Consequently, it is assumed that the surface coverages by these species may be significant and thus need to be included in the site-blocking term of the ketonization rate expression. In contrast, the amount of adsorbed 6-undecanone is assumed to be negligible, because we found that a similar ketone (2-butanone) did not have an effect on the rate of reaction. The rate expression for the ketonization reaction can then be written as Eq. (4), where $k_{f,i}$ is the forward rate constant for reaction i.

$$rate_{ketonization} = \frac{k_{f,keton} \cdot P_{hex-ac}^2}{\left(1 + K_{ads,hex-ac} P_{hex-ac} + K_{ads,water} P_{water} + K_{ads,CO_2} P_{CO_2}\right)^2} \tag{4}$$

Esterification is reported to be catalyzed by acid catalysts [19–21]. In our case, esterification can be considered as a side reaction which occurs on the acidic sites of ceria–zirconia. Even though site-blocking effects have been reported elsewhere for esterification reactions [19], our observations suggested that site-blocking effects are negligible for this reaction at the conditions of the present study, because the rate of esterification increased linearly with the partial pressure of both the reactants (Figs. 6 and 8). Furthermore, the weak nature of the acid sites present on the surface of ceria–zirconia [26] supports the idea that none of the reactants or products of esterification is strongly adsorbed on the catalyst surface for the reaction conditions studied. Accordingly, the esterification reaction is modeled as a reversible reaction taking place on acidic sites in which adsorbed hexanoic acid and 1-pentanol react to form 1-pentylhexanoate and water, with negligible blocking of surface sites by adsorbed species. Thus, the rate expression for the esterification reaction can be written as Eq. (5).

$$rate_{esterification} = k_{f,ester} \cdot P_{hex-ac} P_{1-pentanol} \left(1 - \frac{P_{ester} P_{water}}{P_{hex-ac} P_{1-pentanol} K_{eq,ester}}\right) \tag{5}$$

The model is parameterized by the forward activation energy barriers, E_i, and pre-exponential factors, A_i, for the ketonization and esterification reactions and the binding energies, BE_j, for hexanoic acid, water, and carbon dioxide. The standard state enthalpies and entropies for hexanoic acid, 1-pentanol, water, and carbon dioxide in the gas phase at 448 K were determined from tabulated values [27]. The heat capacity at constant pressure, C_p, was calculated at 448 K and was assumed to be constant. The heat capacity for each species was used to calculate the gas phase thermodynamics at other temperatures. Enthalpy and entropy values for pentylesters derived from other carboxylic acids (pentyl formate, pentyl ethanoate, pentyl propionate, and pentyl butanoate) were extrapolated to obtain the data for 1-pentylhexanoate. In particular, enthalpy, entropy, and heat capacities for other pentylesters were calculated at 448 K. The values were plotted versus the carbon number of the acid part of the ester. The slope and intercept of the plot were used to extrapolate the value for the pentyl ester of hexanoic acid (6 carbon atoms). All thermochemical values are shown in Table 4. The thermodynamic properties for adsorbed species were determined by adjusting the gas phase enthalpies and entropies with the binding energies and translational entropies, respectively. The local entropy values (i.e., rotational and vibrational entropies) of the adsorbed species are calculated by subtracting the three dimensional translational entropy, calculated using Eq. (6), from the gas phase entropy. In Eq. (6) m is the mass of the molecule of interest, h is Plank's constant, k_B is Boltzman's constant and T is the temperature in Kelvin. For simplicity, it is assumed that all of the local entropy is retained by the adsorbed species. Any errors introduced by entropy

Table 4
Thermochemistry for esterification.

	Enthalpy of formation at 448 K (kJ/mol)	Entropy of formation at 448 K (J/mol/K)	Heat capacity at const. pressure at 448 K (J/mol/K)
1-Pentanol	−312	274	183
Hexanoic acid	−520	290	218
Water	−243	165	35
1-Pentylhexanoate	−634	768	371
Carbon dioxide	–	223	43

assumption would be compensated by adjustments to the values of the enthalpies and activation energies fit in the kinetic model.

$$S^{\circ}_{trans,3D} = R\left[\ln\left(\frac{(2\pi m k_B T)^{3/2}}{h^3}\right) + \ln\left[\frac{k_B T}{h}\right] + \frac{5}{2}\right] \quad (6)$$

The enthalpies of the adsorbed species are calculated by adding the binding energy to the gas phase enthalpy for a given molecule. The equilibrium constant, $K_{i,eq}$, can be calculated from the enthalpy and entropy of reaction using Eq. (7). The forward rate constants are calculated using the Arrhenius expression in Eq. (8). The reverse rate constants can be calculated from the equilibrium constant and forward rate constants using Eq. (9).

$$K_{i,eq} = \exp\left(\frac{-\Delta H^{\circ}_i}{RT} + \frac{\Delta S^{\circ}_i}{R}\right) \quad (7)$$

$$k_i = A_i \exp^{\left(\frac{-E_i}{RT}\right)} \quad (8)$$

$$k_{i,rev} = \frac{k_{i,for}}{K_{i,eq}}, \quad (9)$$

The kinetic model was implemented in MATLAB using the material balances for a plug flow reactor. The differential equations that describe the changing gas phase compositions down the length of the reactor are solved using a built-in differential equation solver in Matlab. The activation energies, pre-exponential factors, and binding energies are optimized to fit the experimental data using the nonlinear parameter estimation function 'nlinfit'. For this optimization, the Talwar method for a robust optimization implemented in the MATLAB toolbox was used. The responses used in the parameter estimation algorithm are the ester and ketone flow rates out of the reactor. Confidence intervals (95%) are determined for the optimized parameters using the 'nlparci' function in MATLAB that uses a statistical method based on the asymptotic normal distribution for the parameters estimates.

Based on the experiments shown in Tables 2 and 3, the model was run without an optimization function and the parameters were adjusted manually. These adjusted values for the binding energies of hexanoic acid, water, and carbon dioxide were used as initial guesses for the optimization runs, including all the experiments shown in Table 1.

In the optimization runs, the binding energy of water on the ceria/zirconia surface turned out to be less sensitive than the other parameters for calculating the overall rate. Thus, it was set to the physically reasonable value −96 kJ/mol for the final optimization runs. The model parameters and their confidence intervals determined from the optimization procedure are shown in Table 5. Fig. 6–9 show the whole range of the experimental data and the model predictions obtained with the optimized parameters for the esterification and ketonization reactions.

Examining the confidence intervals for the predicted parameters in Table 5, it can be seen that the proposed kinetic model describes the experimental data well. The calculated confidence intervals are relatively narrow for the activation energies, suggesting that the determined values are appropriate for the conditions tested and modeling assumptions used. This same statement can be made for the binding energies of carbon dioxide and hexanoic acid. To further investigate the validity of the assumption that inhibiting effects of adsorbed species are negligible for the esterification reaction, a site-blocking term (involving adsorbed hexanoic acid) was included in the esterification rate expression. The goodness of the fit did not improve upon addition of this term, thus suggesting that the acid concentrations are too low or the species binding energies are not significantly strong to necessitate the inclusion of site blocking for the esterification reaction in the mod-

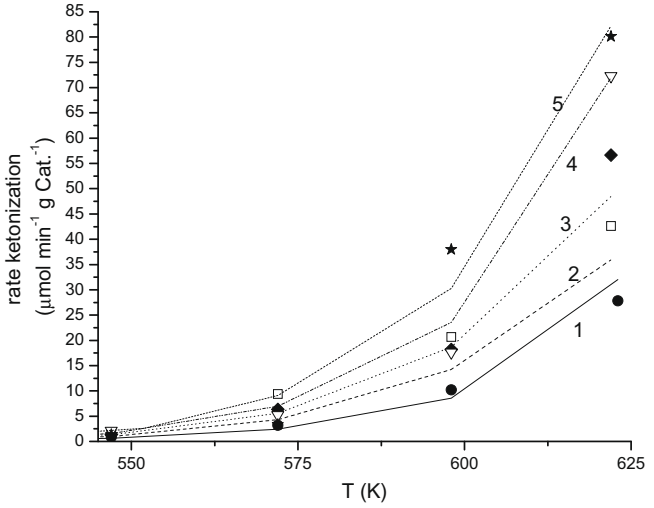

Fig. 7. Experimental data (exp) and simulation (sim) results for ketonization, partial pressure of hexanoic varied (hex ac), partial pressure of 1-pentanol constant at 0.1 atm: (●) 0.05 atm hex ac exp, (1) 0.05 atm hex ac sim, (□) 0.1 atm hex ac exp, (2) 0.1 atm hex ac sim, (♦) 0.15 atm hex ac exp, (3) 0.15 atm hex ac sim, (▽) 0.2 atm hex ac exp, (4) 0.2 atm hex ac sim, (★) 0.3 atm hex ac exp, (5) 0.3 atm hex ac sim.

Table 5
Optimized values of kinetic parameters.

		Optimized value	Lower confidence interval	Upper confidence interval	Unit
Activation energy	Esterification	40.4	39.8	41.0	kJ/mol
	Ketonization	132.2	129.4	135.1	kJ/mol
Pre-exponential factor	Esterification	6.6E+05	5.7E+05	7.4E+05	–
	Ketonization	7.8E+14	7.6E+14	8.0E+14	–
Binding energy	Hexanoic acid	−81.1	−84.1	−78.0	kJ/mol
	Carbon dioxide	−137.9	−139.7	−136.1	kJ/mol
	Water	−96.0	–	–	kJ/mol

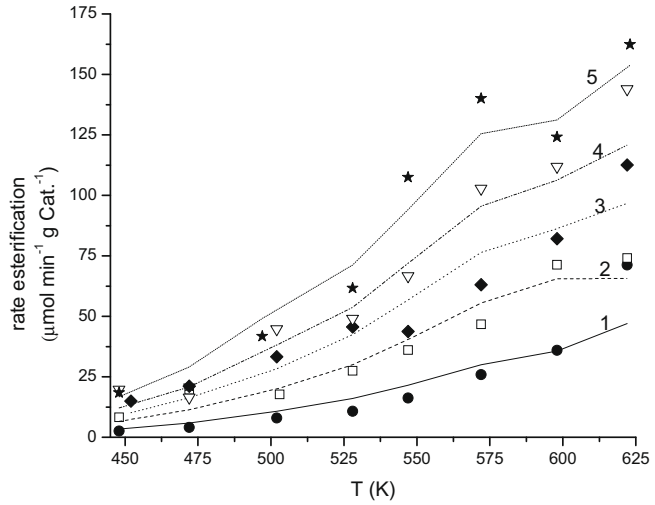

Fig. 8. Experimental data (exp) and simulation (sim) results for ester formation, partial pressure of 1-pentanol (pent) varied, partial pressure of hexanoic acid constant at 0.1 atm: (●) 0.05 atm pent exp, (1) 0.05 atm pent sim, (□) 0.1 atm pent exp, (2) 0.1 atm pent sim, (♦) 0.15 atm pent exp, (3) 0.15 atm pent sim, (▽) 0.2 atm pent exp, (4) 0.2 atm pent sim, (★) 0.3 atm pent exp, (5) 0.3 atm pent sim.

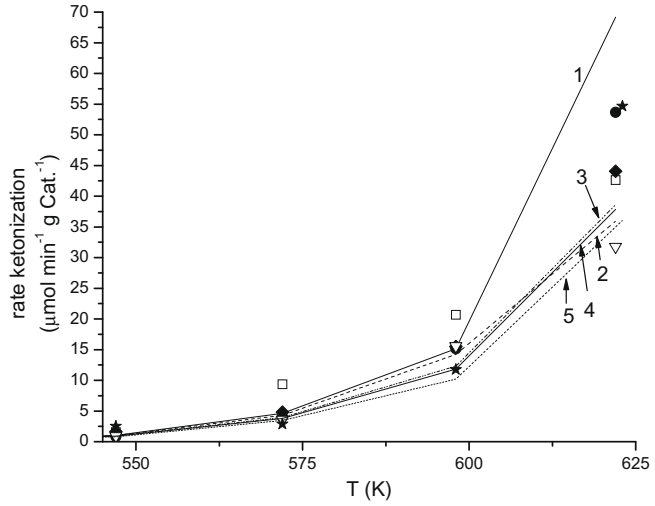

Fig. 9. Experimental data (exp) and simulation (sim) results ketonization, partial pressure of 1-pentanol (pent) varied, partial pressure of hexanoic acid constant at 0.1 atm: (●) 0.05 atm pent exp, (1) 0.05 atm pent sim, (□) 0.1 atm pent exp, (2) 0.1 atm pent sim, (♦) 0.15 atm pent exp, (3) 0.15 atm pent sim, (▽) 0.2 atm pent exp, (4) 0.2 atm pent sim, (★) 0.3 atm pent exp, (5) 0.3 atm pent sim.

el. As seen from the results of the kinetic model, the esterification reaction has a lower activation energy barrier than the ketonization reaction and thus occurs at lower temperatures. The rate of ketonization becomes significant at temperatures higher than approximately 548 K. The value of the ketonization activation energy determined here (132 kJ/mol) is similar to the value reported elsewhere (159 kJ/mol) [25], even though a different catalyst and a different carboxylic acid were used. It has been suggested [25] that for temperatures below 673 K, adsorbed carboxylic acid species appear to have the most significant effect on the rate ketonization, followed by water and then CO_2. From the present study, it was determined that adsorbed CO_2 and water have significant effects on the rate of ketonization, followed by the effect of adsorbed hexanoic acid. However, our study used a different catalyst that is known to adsorb CO_2 strongly. In this respect, results from temperature-programmed desorption studies of ceria oxide have been reported elsewhere [28], showing strong adsorption of CO_2. In particular, a fraction of the adsorbed CO_2 desorbs at a relatively high temperature (860 K). Thus, the high binding energy for CO_2 predicted from the model (Table 5) is consistent with previous studies reported.

The kinetics of the esterification and ketonization reactions are described well with our simple model in a concentration range typical of biomass-upgrading intermediates. Accordingly, this model can then be used to predict the reaction conditions required to upgrade various kinds of biomass-derived feeds over a $Ce_{0.5}Zr_{0.5}O_2$ catalyst, as carboxylic acids are present in various biomass-derived feeds [29]. In this respect, we have employed this ceria–zirconia catalyst to ketonize fully the carboxylic acids and esters present in liquid organic streams derived from the processing of glucose over a Pt–Re/C catalyst [5].

The ketonization of esters, which are an essential intermediate product in many biomass-conversion processes [30], is a more difficult problem compared to the conversion of carboxylic acids, and the literature does not agree about the details of the reaction mechanism [13,14]. One of the suggestions is the intermediate formation of an acid by hydrolysis, which we assume is the predominant pathway in our system. Thus, one approach to convert a large amount of esters to ketones is to provide water with the reaction mixture fed to the reactor. Water, however, decreases the activity of the $Ce_{0.5}Zr_{0.5}O_2$ catalyst, so this approach is not the optimal solution. However, it is possible that biomass-derived intermediate feeds will contain acids and esters, as we have observed in the conversion of glucose over Pt–Re/C. Because of the stronger adsorption of acids on the catalyst surface compared to esters, direct ketonization of esters will not take place as long as acids are present. Thus, ketonization of acids takes place preferentially compared to ketonization of esters. Accordingly, our model does not include the direct ketonization route from esters, which is a limitation. Above 623 K and without presence of acids this reaction becomes essential. Thus, expanding the model for this reaction and for temperatures above 623 K is a goal for future study. Importantly, the water formed by the ketonization of carboxylic acids leads to the subsequent hydrolysis of esters to form carboxylic acids and alcohols, which is followed by the ketonization of these newly formed carboxylic acids. In this way, the coupling between ketonization and hydrolysis reactions (the latter being the reverse of esterification) provides an efficient pathway for the condensation of esters to larger ketones in the temperature range of the present study.

5. Conclusions

The ketonization of carboxylic acids to form ketones was carried out using a feed containing primary alcohols over a ceria–zirconia catalyst. The esterification reaction proceeds more rapidly than the ketonization at lower temperatures, while ketonization becomes the dominant process at the higher temperatures, in good agreement with the higher predicted activation energy for ketonization (132 kJ/mol) compared to the esterification reaction 40 kJ/mol. This difference in activation energy indicates that temperatures higher than approximately 548 K are required to make the ketonization reaction rate competitive with the rate of esterification. Because ketonization is an irreversible reaction, a depletion of hexanoic acid occurs when the rate of ketonization becomes significant. At high ketonization rates, the reverse esterification reaction becomes significant as the equilibrium shifts to replace hexanoic acid that is consumed by ketonization.

Hexanoic acid adsorption on the catalyst surface is an important step in the reaction, and the rate of ketonization shifts from second order to zero order as the partial pressure of hexanoic acid in-

creases. Product inhibition takes place through strong binding of CO_2, and to a lesser extent water, on the basic sites.

Acknowledgments

This work was supported by the U.S. Department of Energy Office of Basic Energy Sciences and the National Science Foundation Chemical and Transport Systems Division of the Directorate for Engineering. C.A. Gaertner thanks the German Academic Exchange Service (DAAD) for a scholarship. J.C. Serrano-Ruiz thanks the Spanish Ministry of Science and Innovation for postdoctoral support. We thank E.L. Kunkes for the temperature-programmed desorption experiment results and for valuable advice. We also thank M. Mavrikakis, R.M. West, D. Wang and E.I. Gürbüz for valuable discussions and technical assistance.

References

[1] C.H. Christensen, J. Rass-Hansen, C.C. Marsden, E. Taarning, K. Egeblad, Chem. Sus. Chem. 1 (2008) 283.
[2] G.W. Huber, A. Corma, Angew. Chem., Int. Ed. 46 (2007) 7184.
[3] G.W. Huber, S. Iborra, A. Corma, Chem. Rev. 106 (2006) 4044.
[4] D.A. Simonetti, J.A. Dumesic, Chem. Sus. Chem. 1 (2008) 725.
[5] E.L. Kunkes, D.A. Simonetti, R.M. West, J.C. Serrano-Ruiz, C.A. Gaertner, J.A. Dumesic, Science 322 (2008) 417.
[6] M. Renz, Eur. J. Org. Chem. (2005) 979.
[7] A. Corma, M. Renz, C. Schaverien, Chem. Sus. Chem. 1 (2008) 739.
[8] K.M. Dooley, A.K. Bhat, C.P. Plaisance, A.D. Roy, Appl. Catal. A 320 (2007) 122.
[9] R. Martinez, M.C. Huff, M.A. Barteau, J. Catal. 222 (2004) 404.
[10] J.C. Serrano-Ruiz, J. Luettich, A. Sepulveda-Escribano, F. Rodriguez-Reinoso, J. Catal. 241 (2006) 45.
[11] D.A. Simonetti, E.L. Kunkes, J.A. Dumesic, J. Catal. 247 (2007) 298.
[12] M. Daturi, C. Binet, J.-C. Lavalley, A. Galtayries, R. Sporken, Phys. Chem. Chem. Phys. 1 (1999) 5717.
[13] R. Klimkiewicz, H. Grabowska, L. Syper, Kinet. Catal. (Translation of Kinetika i Kataliz) 44 (2003) 283.
[14] M. Glinski, W. Szymanski, D. Lomot, Appl. Catal. A 281 (2005) 107.
[15] V. Solinas, E. Rombi, I. Ferino, M.G. Cutrufello, G. Colon, J.A. Navio, J. Mol. Catal. A: Chem. 204–205 (2003) 629.
[16] Y. Kamimura, S. Sato, R. Takahashi, T. Sodesawa, T. Akashi, Appl. Catal. A 252 (2003) 399.
[17] G.A.H. Mekhemer, S.A. Halawy, M.A. Mohamed, M.I. Zaki, J. Catal. 230 (2005) 109.
[18] O. Nagashima, S. Sato, R. Takahashi, T. Sodesawa, J. Mol. Catal. A: Chem. 227 (2005) 231.
[19] D.E. Lopez, K. Suwannakarn, J.G. Goodwin Jr., D.A. Bruce, Ind. Eng. Chem. Res. 47 (2008) 2221.
[20] B. Schmid, M. Doeker, J. Gmehling, Ind. Eng. Chem. Res. 47 (2008) 698.
[21] T.J. Schildhauer, I. Hoek, F. Kapteijn, J.A. Moulijn, Appl. Catal. A 358 (2009) 141.
[22] L. Deng, Y. Fu, Q.-X. Guo, Energy Fuels 23 (2008) 564.
[23] J.I. Gutierrez-Ortiz, B. de Rivas, R. Lopez-Fonseca, J.R. Gonzalez-Velasco, J. Therm. Anal. Calorim. 80 (2005) 225.
[24] R. Pestman, R.M. Koster, A. van Duijne, J.A.Z. Pieterese, V. Ponec, J. Catal. 168 (1997) 265.
[25] S. Rajadurai, Catal. Rev.-Sci. Eng. 36 (1994) 385.
[26] M.G. Cutrufello, I. Ferino, V. Solinas, A. Primavera, A. Trovarelli, A. Auroux, C. Picciau, Phys. Chem. Chem. Phys. 1 (1999) 3369.
[27] C.L. Yaws, Knovel, Yaws' handbook of thermodynamic and physical properties of chemical compounds: Physical, thermodynamic and transport properties for 5000 organic chemical compounds, 2003.
[28] J. Stubenrauch, E. Brosha, J.M. Vohs, Catal. Today 28 (1996) 431.
[29] B.J. Nikolau, M.A.D.N. Perera, L. Brachova, B. Shanks, Plant J. 54 (2008) 536.
[30] D.C. Rennard, P.J. Dauenhauer, S.A. Tupy, L.D. Schmidt, Energy Fuels 22 (2008) 1318.